

## Neutrinoless double electron capture: A tool to search for Majorana neutrinos

Z. Sujkowski\* and S. Wycech†

*Sołtan Institute for Nuclear Studies, Hoża 69, PL-00-681, Warsaw, Poland*

(Received 2 December 2003; published 17 November 2004)

The possibility of observing the neutrinoless double  $\beta$  decay and thus proving the Majorana nature of neutrinos as well as providing a sensitive measure of its mass is a major challenge of today's neutrino physics. As an attractive alternative, we propose to study the inverse process—the radiative neutrinoless double-electron capture ( $0\nu 2EC$ ). The associated monoenergetic photon provides a convenient experimental signature. Other advantages include the favorable ratio of the  $0\nu 2EC$  to the competing  $2\nu 2EC$  capture rates and, very importantly, the existence of a coincidence trigger to suppress the random background. These advantages partly offset the expected longer lifetimes. Rates for the  $0\nu 2EC$  process are calculated. High  $Z$  atoms are strongly favored. A resonance enhancement of the capture rates is expected to occur at an energy release comparable to the  $2P-1S$  atomic level difference. The resonance conditions are likely to be met for decays to excited states in final nuclei. Candidates for such studies are considered. The experimental feasibility is estimated and found encouraging.

DOI: 10.1103/PhysRevC.70.052501

PACS number(s): 23.40.Bw, 14.60.Pq

The existence of massive neutrinos and the Dirac or Majorana nature of these particles are among the most intriguing topics of present-day physics. If a neutrino is a Majorana particle then, by definition, it is identical to its charge conjugate. Thus the neutrino produced in one weak interaction vertex may be absorbed in another one. This leads to the nuclear reaction  $0\nu\beta\beta$

$$(A, Z-2) \rightarrow (A, Z) + e + e \quad (1)$$

(see Fig. 1). Amplitudes for such a process are proportional to the Majorana neutrino mass. While the exact value of the neutrino mass deduced from a successful  $0\nu\beta\beta$  experiment is model dependent, the mere observation of the effect proves unambiguously the Majorana nature of the neutrino as well as the nonconservation of the lepton number. This remains true regardless of the mechanism causing the decay [1,2].

The  $0\nu\beta\beta$  process proceeds via the emission of two correlated  $\beta$  electrons. Its unique signature is that the sum of energies of the two electrons is equal to the total decay energy. The experiments searching for the  $0\nu\beta\beta$  decay can be divided into two categories: the calorimetric experiments, in which the material of the source is usually identical with that of the detector, and the tracking experiments, in which the source and the detector are separate. The former automatically sums up the energies of the charged particles emitted. Large quantities of the material can be used. The main difficulty rests in suppressing the random background. The only way to attain this is by requiring extreme shielding conditions as well as the extreme purity of the detector, of the detector housing and of the surrounding material. The tracking detectors, counting the two electrons in coincidence, are somewhat less sensitive to the background. On the other

hand, there are practical difficulties in handling the necessarily large amount of the source material, on the order of tons, in the form of thin sheets sandwiched between the detectors. The detectors in both kinds of experiments must fulfill the high-resolution requirements. Otherwise the  $0\nu\beta\beta$  peak in the sum spectrum will not be discernible from the dominating continuous physical background due to the

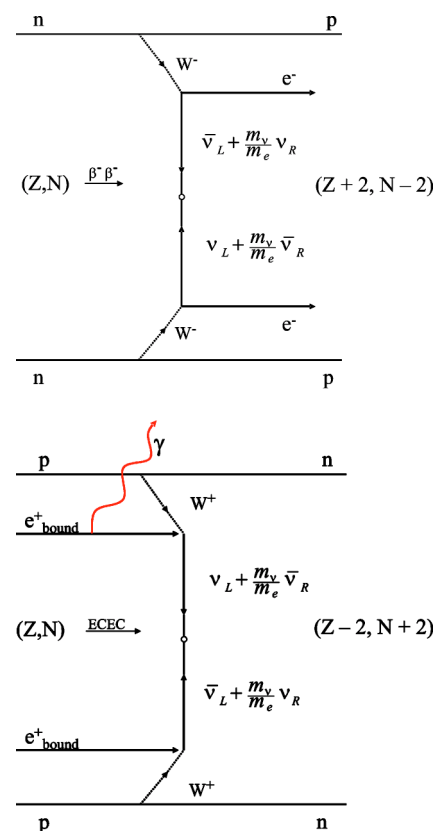


FIG. 1. Diagrams for the  $0\nu$  double beta decay and double-electron capture processes.

\*Email address: sujkow@fuw.edu.pl

†Email address: wycech@fuw.edu.pl

$2\nu\beta\beta$  decay. For the description of the problems involved we refer to reviews [2–6].

We suggest studying the inverse of neutrinoless double  $\beta$  decay, i.e., the neutrinoless double-electron capture. The excess energy is carried away by a photon. Crude estimates [7] for such a radiative process are encouraging, suggesting feasible experiments. These are discussed in the next section on the basis of a theory of the radiative capture adapted to the double-electron capture case. The point of special interest is the resonant effect that occurs when the photon energy equals the energy of atomic  $2P-1S$  transition. In fortunate situations this effect may strongly enhance the  $0\nu\beta\beta$  rates.

There are several experimental advantages of the radiative electron capture process:

- (i) The monoenergetic photon escapes easily from fairly thick layers of the source material without energy degradation.
- (ii) The source can be separate from the detector.
- (iii) The physical background due to the competing  $2\nu\beta\beta$  process is low [8].
- (iv) The photon emission is followed by that of the  $K$  x ray (this provides a precious coincidence trigger to suppress the overwhelming random background).
- (v) Low decay energies are favored. Decays to excited states can thus be considered in realistic experiments in contrast to the  $\beta\beta$  decays. The  $\gamma$  transitions which follow offer yet another characteristic coincidence trigger.

The price to pay is a sizable reduction of the transition rates. The experimental questions and the optimal choice of the isotopes are discussed in the final sections.

The dominant amplitudes for the radiative double-electron capture can be factorized into weak-nuclear, weak-leptonic, and radiative factors [9–11]. The expressions for radiative factors presented below are based on the theory for the radiative single-electron capture process [12,13].

The amplitude for the  $0\nu\beta\beta$  decay from the (*atom* + *nucleus*) ground state  $|0\rangle$  to a final nuclear state  $N_f$  and final two-electron state  $n_f$  is

$$R_{0\nu}^{\beta\beta} = \langle 0 | H_w | n_f, N_f \rangle. \quad (2)$$

This differs from the amplitude for the double-electron capture

$$R_{0\nu}^{cc} = \langle \bar{n}_f, N_f | H_w | 0 \rangle \quad (3)$$

by the electron wave functions. Here  $\bar{n}_f$  denotes two-electron holes in the final atom (say  $1S, 2S$  or  $1S, 2P$ ). The reversed transition cannot be tested in the same nucleus and  $R_{0\nu}^{cc}$  does not correspond to a real physical transition. Assuming the radiative process instead, we can write the corresponding amplitudes in the second order perturbation theory, to the leading order in the radiative interaction  $H_\gamma$ , as

$$R_{0\nu}^\gamma = \sum_{n_i, N_i} \langle n_f, N_f | H_\gamma | n_i, N_i \rangle \frac{\langle n_i, N_i | H_w | 0 \rangle}{E - E(n_i) - E(N_i)}, \quad (4)$$

where  $H_w$  is the weak interaction describing the neutrinoless process of Fig. 1. Intermediate states  $|n_i, N_i\rangle$  in the radiative process may involve ground and excited nuclear states. Only

the electron is considered to radiate as the  $\gamma$  emission by the nucleus is unlikely [14,10].

We look first for the transitions which conserve the nuclear angular momentum ( $0^+ \rightarrow 0^+$ ) as these offer the largest nuclear matrix elements. The final photon and its spin is generated by the electron radiation. Two basic processes are possible.

(a) One of the electrons captured from the initial atomic state  $n_{ini}$  radiates while it propagates towards the nucleus.

(b) Two electrons are captured in a virtual process which generates a final atom with two electron holes. This final atom radiates and one of the holes is filled.

Process (a) is standard in the single-electron radiative captures. The description of electron propagation involves the electron Coulomb Green's functions [12,13]. The two-electron capture requires some modifications. To conserve the angular momentum, for one electron in a  $1S$  state, the other one must be in a higher  $nS$  state. The transition is of the magnetic type. The electron wave functions must be antisymmetrized.

Process (b) is less important in general. However, for the small photon energy  $Q$  the virtual two-electron-hole state may be degenerate to the final atom-photon state [see below, Eq. (12); see also Refs. [15–17]]. This leads to a singularity in  $R_{0\nu}^\gamma$ . The most interesting situation occurs for  $Q = E(2P) - E(1S)$ , i.e., when the final photon resonates with the  $2P-1S$  transitions in the final atom. The capture rate is enhanced up to the limit given by the natural  $K-L$  linewidths.

The cases (a) and (b) require different descriptions. In the simplest theory of Majorana neutrinos [9,10] the matrix element  $R_{0\nu}^{cc}$  is

$$R_{0\nu}^{cc} = 2 \left( \frac{G}{\sqrt{2}} \right)^2 \int d\mathbf{x} d\mathbf{y} \langle J_N(\mathbf{x})^\rho m_\nu h_\nu(\mathbf{x} - \mathbf{y}) J_N(\mathbf{y})^\sigma \rangle \times \Psi(n_1, \mathbf{x}) \gamma_\rho (1 - \gamma_5) \gamma_\sigma \bar{\Psi}^C(n_2, \mathbf{y}). \quad (5)$$

The nuclear weak currents are denoted by  $J_N$  and the effect of neutrino propagation is included into the “neutrino potential” with  $h_\nu(r) \approx \exp(-qr)/r$ , where  $q$  is an average momentum carried by the neutrino (the closure approximation over nuclear states is used here). The projection on the left-handed intermediate neutrino brings about the neutrino mass factor  $m_\nu$ . The electronic part of this formula contains atomic wave functions  $\Psi$  and the charge conjugates  $\Psi^C$ . For the  $0^+ \rightarrow 0^+$  transitions the nuclear part is reduced to Fermi and Gamow-Teller matrix elements defined by  $M_F = \langle 0 | h_\nu | 0 \rangle$  and  $M_{GT} = \langle 0 | h_\nu \sigma_1 \sigma_2 | 0 \rangle$ . These enter via a combination  $M^{0\nu} = M_{GT} - (g_V/g_A)^2 M_F$  and in this way the transition matrix element (3) is brought to the form

$$R_{0\nu}^{cc} = 2 \left( \frac{G}{\sqrt{2}} \right)^2 M^{0\nu} m_\nu [\Psi(n_1, 0) S(1, 2) \Psi(n_2, 0)]_A, \quad (6)$$

which resembles the standard  $\beta\beta$  decay expression [9]. The electron wave functions are required in the nuclear region. These are  $\Psi(n_e, 0)\hat{u}$ , where  $\Psi(n_e, 0)$  is the radial part of the large component and  $\hat{u}$  is the Dirac spinor. The spin matrix element is given by  $S(1, 2) = u(n_1)(1 + \gamma_5)\bar{u}^C(n_2)$ . In Eq. (6)

the electron wave function is to be antisymmetrized. For two  $1S$  electrons this involves the antisymmetric spin zero combination of spinors which compensates an “inner antisymmetry” built into operator  $S(1,2)$  by the charge conjugation.

To describe the radiative capture of the type (a), one function  $\Psi$  is to be replaced by some function  $\Psi_\gamma$  which takes care of the photon emission and electron propagation. In Eq. (4), in coordinate representation, this function is given by the expression

$$\Psi_\gamma(\mathbf{r}, n_{ini}) = \sum_{n_i} \frac{(\mathbf{r}|n_i)(n_i|H_\gamma|n_{ini})}{E - E(n_i) - E(0)}, \quad (7)$$

which involves the sum over the continuum and discrete states of the electron, i.e., the Dirac Green’s function in the external Coulomb field of the nucleus (Glauber and Martin [12,13]). This solution is now implemented into Eq. (4) to give the radiative amplitude

$$R_{0\nu}^\gamma = 2 \left( \frac{G}{\sqrt{2}} \right)^2 m_\nu M^{0\nu} [\Psi(n_1, 0) S(1, 2, \vec{\epsilon}, \vec{Q})_\gamma \Psi(n_2, 0)_\gamma]_A \quad (8)$$

where the leptonic spins and the photon polarization  $\epsilon$  enter the last term

$$S(1, 2, \vec{\epsilon}, \vec{Q})_\gamma = \frac{\sqrt{\alpha}}{2m_e} [u(n_1) [iA(Q) \vec{\sigma} \vec{\epsilon} \times \vec{Q} - B(Q) \vec{\epsilon} \vec{Q}] \times (1 + \gamma_5) \bar{u}^C(n_2)]. \quad (9)$$

For the discussion of  $A(Q)$  and  $B(Q)$  we refer to Ref. [13]. If  $Q \approx m_e$  then  $A, B$  are close to unity for both the  $1S$  and  $2S$  electrons. The spin conservation requires the two electrons to be in the symmetric spin and antisymmetric space combinations. This causes cancellations at small  $Z$ . Otherwise the effect of symmetrization is small.

The rate for the radiative no-neutrino process is now

$$\Gamma^{0\nu\gamma}(Q) = \sum_{pol} \int \frac{2\pi d\mathbf{k}}{(2\pi)^3 2k} \delta(k - Q) |R_{0\nu}^\gamma|^2, \quad (10)$$

to be summed over photon polarization and possible electron pairs. The result is

$$\Gamma^{0\nu\gamma} = \left( \frac{G}{\sqrt{2}} \right)^4 \left[ M_{GT} - \left( \frac{g_V}{g_A} \right)^2 M_F \right]^2 (m_\nu/m_e)^2 \times |\Psi(1S, 0) \Psi(2S, 0)|^2 \frac{Q}{2\pi} \sum_{pol} \langle S(n_1, n_2, \vec{\epsilon}, \vec{Q})_\gamma \rangle^2, \quad (11)$$

where the summation over the spin factor  $\langle S \rangle$  is to be taken. This factor takes care of the angular momentum conservation. The best possibility is the  $1S, 2S$  pair capture accompanied by a magnetic photon transition. This rate is scaled by the  $S$  electron wave function at the nucleus. One has  $\Psi(n_{1S}, 0)^2 = (Zm_e\alpha)^3 f_s^2 / \pi$ , where the factor  $f_s$  comes from the weak singularity of Dirac atomic wave function. Averaged over the nuclear volume it becomes  $f_s = (2RZm_e\alpha)^{\lambda-1}$  with  $\lambda = \sqrt{1 - (Z\alpha)^2}$  and the nuclear radius  $R$ . The  $Z^6$  factor arises and thus one is interested in the heaviest possible at-

TABLE I. The radiative neutrino-less capture rates from the  $1S, 2S$  states [ $1/\gamma$ ],  $m_\nu = 1$  eV.

Atom	abundance %	$Q$ [keV]	$\Gamma$ ( $2S, 1S$ )
$^{92}_{42}\text{Mo}$	15.84	1628(5)	$2 \times 10^{-32}$
$^{108}_{48}\text{Cd}$	0.88	241(7)	$1 \times 10^{-31}$
$^{144}_{62}\text{Sm}$	3.07	1730(4)	$1 \times 10^{-31}$
$^{162}_{68}\text{Er}$	0.14	1781(4)	$2 \times 10^{-30}$
$^{180}_{74}\text{W}$	0.12	66(5)	$2 \times 10^{-31}$
$^{196}_{80}\text{Hg}$	0.15	729(3)	$4 \times 10^{-30}$

oms. There the relativistic singularity enhances the rate further.

At smaller  $Q$  the capture amplitude indicates an interesting structure. The electron propagator in Eq. (7) has a pole at  $Q = |E(1S) - E(2P)| \equiv Q_{res}$ . To elucidate the atomic physics involved in this radiation process, amplitude (4) is presented in terms of the initial state

$$|\Psi_{ini}\rangle = |0\rangle + \sum_{n_i, N_i} \frac{(n_i, N_i | H_w | 0)}{E - E(n_i) - E(N_i)} |n_i, N_i\rangle, \quad (12)$$

where  $E = E_N(0) + E_{atom}(0)$  is the initial energy of the system composed of the nuclear part  $E_N$  and the atomic component  $E_{atom}$ . Equation (12) describes the virtual transitions of the initial state  $|0\rangle$  under weak interactions which include virtual two electron capture states. Some of these states may be degenerate with the final atom+photon state to within the natural width of the  $K-L$  line. Rate enhancements of the order of  $10^4 - 10^6$  may be obtained. In the single-electron description by Glauber and Martin, the electron propagator in Eq. (7) has a pole at  $Q = |E(1S, Z) - E(2P, Z)| \equiv Q_{res}(Z)$  where  $Z$  refers to the initial atom. In the many electron process considered here we use the energy levels for *final* ( $Z-2$ ) atom (see also Ref. [17]). We obtain

$$\Gamma^{0\nu\gamma}(Q) = \frac{\Gamma^r(2P \rightarrow 1S)}{[Q - Q_{res}(Z-2)]^2 + [\Gamma^r/2]^2} |R_{0\nu}^{cc}|^2, \quad (13)$$

where  $\Gamma^r$  is the radiative width of the final two-electron-hole atom. We use the experimental energy values for the  $Z-2$  atoms corrected for the screening differences in the ionized atoms; the combined width is  $3\Gamma^r(1S) + \Gamma^r(2P)$  similarly as for the hypersatellite  $K^h$  x-ray spectra.

The usual choice for targets in the double  $\beta$  decay is motivated by the phase space that favors large energy release (roughly  $Q_{\beta\beta}^5$  dependence). In contrast, the phase-space dependence of the double-electron capture Eq. (11) is rather weak and the radiative factors favor small  $Q$ . Two capture situations can be considered. At  $Q$  larger than the electron mass, the “magnetic” radiative capture of  $1S, 2S$  pair dominates. The calculated rates (Table I) are based on values  $M_{GT} \approx 0.6/\text{fm}$  and  $M_F/M_{GT} \approx -0.3$  obtained in typical  $\beta\beta 0\nu$  reactions in a number of nuclei [18,19]. These values give a crude estimate also for the  $0\nu cc$  processes, although some calculations indicate a larger coupling [20].

At small  $Q$  the capture amplitude is given by the resonant

TABLE II. The resonant situations. The radiative neutrinoless capture rates per year  $R/y$ , and per year and ton of the isotope  $R/y \cdot \text{ton}$ ,  $m_\nu=1$  eV. The uncertainties of  $R/y \cdot \text{ton}$  are due to  $1\sigma$  errors in the mass determination.  $Q$ , photon energies;  $Q_r$ , the resonant energies;  $Q_x, Q_\gamma$ , energies of accompanying x-ray,  $\gamma$ -ray photons;  $E^*$ , excitations of final nuclei (keV); f.st., final state; int. st., initial state.

Atom	$^{112}_{50}\text{Sn}$	$^{136}_{58}\text{Ce}$	$^{152}_{64}\text{Gd}$	$^{162}_{68}\text{Er}$	$^{164}_{68}\text{Er}$	$^{180}_{74}\text{W}$
abnd.%	1.01	0.19	0.20	0.14	1.56	0.13
f.st.	$0_2^+, 1S, 2P$	$0_3^+, 1S, 2P$	g.s., $1S, 2P$	$1^+, 1S, 2P$	g.s., $2S, 2P$	g.s., $1S, 2P$
int.st.	$0_2^+, 1S, 1S$	$0_3^+, 1S, 1S$	g.s., $1S, 2S$	$1^+, 1S, 1S$	g.s., $2S, 2S$	g.s., $1S, 1S$
$\Delta M$	1919.5(4.6)	2418.9(13)	54.6(3.5)	1843.8(3.9)	23.3(3.9)	144.4(4.5)
$E^*$	1870.9	2315.4		1745.5		
$Q$	18.0(4.6)	60.13	39.7(3.5)	36.1(3.9)	6(4)	68.6(4.5)
$Q_r$	23.8	33	39.7	46.6	1	56.3(4.5)
$Q-Q_r$	-5.8(4.6)	27(13)	0.04(3.5)	-10.5(3.9)	5(4)	12.3(4.5)
$Q_x$	23	32	6.5	46	6.5	55
$Q_\gamma$	1253.4	1496.9		1665.1		
	617.6	818.5		80.6		
$R/y$	$7 \times 10^{-30}$	$2 \times 10^{-30}$	$2 \times 10^{-25}$	$1 \times 10^{-28}$	$2 \times 10^{-32}$	$3 \times 10^{-28}$
$R/y \cdot \text{t}$	$1 - 10^{-2}$	$10^{-1} - 10^{-3}$	$10^3 - 10^{-1}$	$1 - 10^{-1}$	$10^{-1} - 10^{-3}$	$3 - 0.2$

conditions. Several candidates for such a resonant capture may be found. Examples are given in Table II. The region of practical interest is limited to  $Q < 80$  keV. Such conditions are likely to be met in the transitions to the excited states of the final nuclei. The rate predictions are hampered by the poor knowledge of mass differences. Because of the sharp atomic resonances, a few keV mass-uncertainty results in rates changing by several orders (see. Table II). The atomic ground state (g.s.) mass differences  $\Delta M$  are taken from Refs. [21,22] and the  $Q$  values are  $\Delta M$  reduced by the two-electron-hole excitation energies. The precision needed is well below 1 keV.

The experimental signature for the double-electron capture in the resonance conditions will be the  $KX-K^h$  x-ray coincidence and, in the case of decays to excited states, the triple coincidence with the gamma rays deexciting these states. The  $K^h$  line has a measurable energy shift. The experimental feasibility arguments have to include the decay rate and the cost estimates. Leaving the cost arguments aside and assuming one ton of the source material with 100% isotopic purity and the correspondingly larger amount of a high-resolution detector (e.g., a multilayered source-detector sandwich for x-ray detection combined with the medium resolution larger  $\gamma$ -ray detectors), it seems possible to design feasible experiments for the  $0\nu$  double-electron capture process. The count rates expected depend strongly on the energy difference with respect to the resonance value (see Table II). The  $^{112}\text{Sn}$  isotope indicated in Ref. [17] as the best choice, now with the the recent mass determination, seems less profitable. Much higher decay rates can be expected for  $^{152}\text{Gd}$  and  $^{164}\text{Er}$  g.s.  $\rightarrow$  g.s. decays. However, there are no convenient experimental signatures in these transitions. The best signatures are offered in the cases of decays to excited states (e.g.,  $^{112}\text{Sn}$ ,  $^{136}\text{Ce}$ , or  $^{162}\text{Er}$ ) where there are characteristic high energy  $\gamma$  rays in addition to the  $k_\alpha$  x rays and the resonant transitions.

One advantage of the  $0\nu\gamma$  process is a favorable ratio of

the signal to the physical background generated by the dominant  $\nu\nu\gamma$  channel. Here, we briefly estimate this ratio defined as

$$R_{S/B} = \frac{\Gamma^{0\nu\gamma}(Q)}{\Gamma^{\nu\nu\gamma}N_D}, \quad (14)$$

where  $N_D$  is the fraction of photons from the dominant  $\nu\nu\gamma$  decay mode emitted into the region from the end of the spectrum  $Q$  down to  $Q-D/2$  and  $D$  is the photon energy resolution. More details may be found in Ref. [8]. For easier comparison the two-neutrino radiative rate is presented in terms of the no-neutrino radiative rate  $\Gamma^{0\nu\gamma}(k_\gamma)$ , given by Eq. (11) or Eq. (13), as a function of the photon energy

$$\Gamma^{\nu\nu\gamma} = \int dL \delta(Q - \Sigma k_i) R_N^2 \Gamma^{0\nu\gamma}(k_\gamma) \frac{(2\pi)^2}{k_\gamma}, \quad (15)$$

where the phase-space element  $dL = (2\pi d\mathbf{k}_\gamma d\mathbf{k}'_\nu) / [(2\pi)^9 8k_\gamma k'_\nu]$  and  $R_N = (4\pi M^{2\nu}) / (M^{0\nu} m_\nu)$  is a dimensionless ratio of the nuclear two-neutrino and no-neutrino matrix elements. Typical values  $M^{2\nu} \approx 1$ ,  $M^{0\nu} \approx 1/\text{fm}$  follow from nuclear model calculations [3,10]. To obtain  $R_{S/B}$ , expression (15) is presented as an integral over the photon energy distribution  $\Gamma^{\nu\nu\gamma} = \int_0^Q W(k_\gamma) dk_\gamma$  and the background contribution becomes

$$\Gamma^{\nu\nu\gamma} N_D = \int_{Q-D/2}^Q W(k_\gamma) dk_\gamma. \quad (16)$$

Formula  $W(k_\gamma) = (Q - k_\gamma)^3 \Gamma^{0\nu\gamma}(k_\gamma) R_N^2 / 6(2\pi)^4$  follows from Eq. (15). This indicates a cubic cutoff at the end of the spectrum due to the phase space. The ratio  $R_{S/B}$  is now given by the interplay of this cutoff and the energy dependence of  $\Gamma^{0\nu\gamma}(k_\gamma)$ .

First, we consider the magnetic type transition related to the  $1S, 2S$  electron capture. For characteristic values  $Q = 1$  MeV and  $m_\nu = 1$  eV, one obtains  $\Gamma^{0\nu\gamma} / \Gamma^{\nu\nu\gamma} = 5 \times 10^{-5}$ .



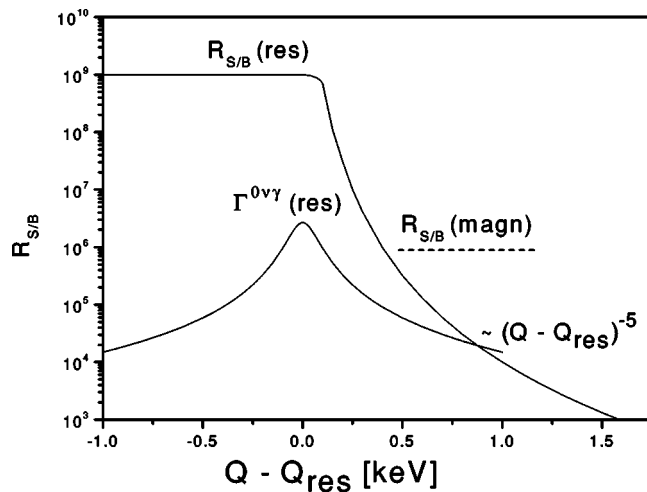


FIG. 2. Schematic plot for the signal/physical background ratios:  $R_{S/B}(\text{res})$ : continuous line for the resonant transition, and  $R_{S/B}(\text{magn})$ : dashed line for the magnetic transition. The rate dependence  $\Gamma^{0\nu\gamma}(\text{res})$  vs  $(Q - Q_{\text{res}})$  is shown in arbitrary units to indicate the resonance width.

The photon energy resolution  $D=3$  keV would yield a very convenient  $R_{S/B}=2 \times 10^9$ . The case of resonant electron captures is more involved due to the rapid energy dependence in  $\Gamma^{0\nu\gamma}(k_\gamma)$ . The result is plotted in Fig. 2. The  $Q \leq Q_{\text{res}}$  situation is very favorable and  $R_{S/B}$  is about  $10^9$ . For  $Q > Q_{\text{res}} + \Gamma^\gamma$  the  $R_{S/B}$  falls down as  $[Q - Q_{\text{res}}]^{-5}$ . At  $Q - Q_{\text{res}} = 1$  keV, the ratio is still very convenient,  $R_{S/B} \approx 10^4$ , but the condi-

tions deteriorate quickly with the increasing energy separation.

The random background (RB) varies with the source material. Crudely, the effect/RB ratios are expected to be improved in comparison to the calorimetric  $\beta^-\beta^-$  experiments [5] by a factor of between 10 and 1000, depending on the x-ray and the  $\gamma$ -ray coincidence trigger.

We conclude that detecting the neutrinoless double beta process of any kind, be it  $\beta^-$ ,  $\beta^+$ , or electron capture, will mean discovering the lepton number nonconservation and proving the Majorana nature of neutrinos. It will also provide a sensitive measure of the neutrino mass, thus giving answers to some of the most urgent questions of physics today. This search calls for a massive, diversified experimental as well as theoretical effort. The radiative neutrino-less double-electron capture proposed in this work is a valid alternative to double  $\beta^\pm$  emission, with several experimental advantages. The predicted resonance rate enhancement makes this search plausible. Exact rate predictions require precise measurements of masses and likewise calculations of nuclear matrix elements. The former are feasible with modern techniques [23,22]. The latter are strongly assumption dependent. The consensus [24] is that they can be trusted to about a factor of 3. One way to minimize this uncertainty is to carry out measurements for several nuclear species, preferably on both sides of the mass parabolas. Thus the double-electron capture search can be considered not only as an attractive alternative to the double  $\beta^-$ . Assuming both kinds of experiments are successful, it will also provide a much needed complementary piece of information.

- [1] R.N. Mohapatra and P.B. Pal, *Massive Neutrinos* (World Scientific, Singapore, 2001).
- [2] F. Boehm and P. Vogel, *Physics of Massive Neutrinos* (Cambridge University Press, Cambridge, 1987).
- [3] H. Ejiri, *Phys. Rep.* **338**, 265 (2000).
- [4] S. Elliott and P. Vogel, *Annu. Rev. Nucl. Part. Sci.* **52**, 15 (2002).
- [5] H.V. Klapdor-Kleingrothaus, *Part. Nucl. Lett.* **1**, 20 (2001); H.V. Klapdor-Kleingrothaus *et al.*, *Phys. Lett. B* **586**, 198 (2004).
- [6] Z. Sujkowski, *Acta Phys. Pol. B* **34**, 2207 (2003).
- [7] Z. Sujkowski and S. Wycech, *Acta Phys. Pol. B* **33**, 471 (2002).
- [8] S. Wycech and Z. Sujkowski, *Acta Phys. Pol. B* **35**, 1223 (2004).
- [9] M. Doi, T. Kotani, and E. Takasugi, *Prog. Theor. Phys. Suppl.* **83**, 1 (1985); M. Doi and T. Kotani, *Prog. Theor. Phys.* **89**, 139 (1993).
- [10] J.D. Vergados, *Nucl. Phys.* **218**, 109 (1983).
- [11] J. Suhonen and O. Civitarese, *Phys. Rep.* **300**, 123 (1998).
- [12] R.J. Glauber and P.C. Martin, *Phys. Rev.* **104**, 158 (1956).
- [13] P.C. Martin and R.J. Glauber, *Phys. Rev.* **109**, 1307 (1958).
- [14] T. Tomoda, *Rep. Prog. Phys.* **54**, 53 (1991).
- [15] R.G. Winter, *Phys. Rev.* **100**, 142 (1955).
- [16] H.M. Georgi, S.L. Glashow, and S. Nussinov, *Nucl. Phys.* **B193**, 297 (1981).
- [17] J. Bernabeu, A. de Rujula, and C. Jarlskog, *Nucl. Phys.* **B223**, 15 (1983).
- [18] J. Suhonen, *Phys. Rev. C* **62**, 042501(R) (2000).
- [19] F. Simkovic *et al.*, *Phys. Rev. C* **64**, 035501 (2001).
- [20] S. Stoica and H.V. Klapdor-Klaingrothaus, *Eur. Phys. J. A* **17**, 529 (1998).
- [21] V.I. Tretyak and Y.G. Zdesenko, *At. Data Nucl. Data Tables* **66**, 83 (2002).
- [22] G. Audi, A.H. Wapstra, and C. Thibault, *Nucl. Phys.* **A729** 337 (2003).
- [23] T. Fritioff *et al.*, *Eur. Phys. J. A* **15**, 423 (2002).
- [24] *Proceedings of the 1st Yamada Symposium on Neutrinos and Dark Matter in Nuclear Physics, Nara, Japan, 2003*, edited by H. Ejiri and I. Ogawa (unpublished).